

Multicore vortex solitons in cubic–quintic nonlinear media with a Bessel lattice potential

Di Wu ^{a,b,1}, Junhao Li ^{a,c,1}, Xi Gao ^{a,c}, Yi Shi ^{a,c}, Yuan Zhao ^{a,b,1}, Liangwei Dong ^d, Boris A. Malomed ^{e,1}, Ni Zhu ^{a,f,*}, Siliu Xu ^{a,b,1}

^a Key Laboratory of Optoelectronic Sensing and Intelligent Control, Hubei University of Science and Technology, Xianning, 437100, China

^b School of Biomedical Engineering and Imaging, Xianning Medical College, Hubei University of Science and Technology, Xianning 437100, China

^c School of Electronic and Information Engineering, Hubei University of Science and Technology, Xianning, 437100, China

^d Department of Physics, Zhejiang University of Science and Technology, Hangzhou, 310023, China

^e Instituto de Alta Investigación, Universidad de Tarapacá, Casilla 7D, Arica, Chile

^f School of Basic Medical Sciences, Xianning Medical College, Hubei University of Science and Technology, Xianning 437100, China



ARTICLE INFO

Keywords:

Vortex solitons

Light bullets

Competing nonlinearities

Bessel lattices

Stability

ABSTRACT

We propose a scheme to explore the existence, propagation, and manipulations of two-dimensional (2D) spatial multicore vortex solitons (VSs) and three-dimensional (3D) spatiotemporal vortex light bullets (VLBs) in media with the competing cubic–quintic nonlinearity, confined by azimuthally modulated Bessel lattices. Control parameters of the system include the cubic and quintic nonlinearity coefficients, integer azimuthal-modulation index (which is taken equal to the order of the Bessel function), and the lattice depth. Stable necklace- and ring-shaped VSs and VLBs with topological charges $m = 1, 2$, and 3 are found in the system, as well as unstable ones for higher values of m . Radii of the 2D VSs and 3D VLBs increase with the growth of m . The lattice depth produces a weaker effect onto the stability of the 3D VLBs in comparison to the 2D VSs. The results provide a novel approach for creating stable VSs and VLBs with higher topological charges.

1. Introduction

The generation, propagation, and interactions of vortices in nonlinear systems have been studied in diverse areas of physics, such as nonlinear optics [1,2], Bose–Einstein condensates (BECs) [3] (including spin–orbit-coupled matter waves [4,5]), quantum droplets [6–8], hydrodynamics [9], laser cavities [2], electron beams [10], etc. Vortex solitons (VSs), characterized by screw phase dislocations embedded in localized ring-shaped beams, exist in systems exhibiting focusing nonlinearities [1,2]. However, these solitons often represent higher-order excited states, making them highly susceptible to azimuthal modulation instabilities that lead to their destruction or transition into ground-state (zero-vorticity) solitons [11,12]. In particular, in media with the Kerr or saturable nonlinearity, the azimuthal instability usually breaks VSs into many fragments, which are similar to the ground-state solitons. Experimental observations have confirmed these phenomena in various contexts [13,14].

Several physical settings have been theoretically elaborated to solve the problem of multidimensional solitons and the azimuthal instability [15–17]. Stable VSs [18,19], semidiscrete optical vortex

droplets [20], and vortex light bullets (VLBs) [21] have been predicted theoretically in quasi-phase-matched photonic crystals with quadratic nonlinearity [22–24]. In homogeneous media, combined quadratic-cubic [25] and cubic–quintic [26,27] nonlinearities can effectively suppress azimuthal instability. Alternatively, confined systems, such as graded-index optical fibers [28], nonlinear photonic crystals with defects [29], linear and nonlinear optical lattices [30], and optical lattices with defects [31], can support stable VLBs. Notably, stable 2D VSs and 3D VLBs have been predicted in Rydberg electromagnetically-induced-transparency systems [32–35]. Experimentally, robust nonlinear vortex modes have been observed in cubic–quintic and saturable media [36,37].

The incorporation of lattice potentials into nonlinear media can significantly enhance the stability of localized wave modes in Bose–Einstein condensates (BECs) [38,39] and optical VSs [40–44]. In particular, axially-symmetric structures in the form of Bessel lattices have drawn considerable interest [45]. This lattice can be induced by non-diffracting Bessel beams, which were created experimentally with the help of computer-generated holograms [46] or conical prisms [47].

* Corresponding authors.

E-mail addresses: zhuni@whu.edu.cn (N. Zhu), xusiliu1968@163.com (S. Xu).

¹ The authors contribute equally in this work.

Such lattices can also be generated in photorefractive crystals by means of the phase-imprinting technique [48,49]. Theoretical predictions, based on numerical simulations [50–53] and physics-informed neural networks [54,55], and experimental observations [46] have confirmed the existence of various types of 2D VSs and 3D VLBs in modulated Bessel lattices.

Despite the above-mentioned advancements, the understanding of 2D VSs and 3D VLBs formed in optical lattices with competing nonlinearities remains inadequate. The aim of this paper is to produce stable 2D VSs and 3D VLBs in azimuthally modulated Bessel lattices combined with the cubic–quintic nonlinearity. Control parameters of the resulting system are the cubic and quintic nonlinearity coefficients, γ_1 and γ_2 , the order of the Bessel lattice (integer n), and the lattice depth (p). They determine the distribution and stability range of 2D VSs and 3D VLBs carrying various topological charges (winding numbers). To produce stable 2D VSs and 3D VLBs, the signs of the cubic and quintic nonlinearity must be opposite. The multicore VSs and VLBs are shaped as rings and necklaces, as determined by the order of the Bessel lattice.

The following material is structured as follows: the model is formulated in Section 2, results of the systematic investigation of the VSs and VLBs are reported in Section 3, and the paper is concluded by Section 4.

2. The model

We consider the propagation of light along the z direction in a medium combining the self-focusing cubic and self-repulsive quintic nonlinearities. The scheme of this system is shown in Fig. 1(a), where a probe beam is shone onto a photorefractive crystal. In this setting, the propagation of envelope ψ of the light wave is governed by the nonlinear Schrödinger equation (NLSE):

$$i\frac{\partial\psi}{\partial z} = -\frac{1}{2}\nabla^2\psi - \gamma_1|\psi|^2\psi - \gamma_2|\psi|^4\psi - pV(x, y)\psi. \quad (1)$$

The longitudinal z and transverse x, y coordinates are scaled to the diffraction length kr_0^2 and input beam width r_0 , where $k = 2\pi/\lambda$ is the wavenumber and λ the wavelength. Laplacian $\nabla^2 = \nabla_{x,y}^2 \equiv \partial^2/\partial x^2 + \partial^2/\partial y^2$ represents the paraxial-diffraction operator acting on the transverse spatial coordinates x and y . In the case of VLBs (alias vortex spatiotemporal solitons), temporal variable $T = t - z/V_0$ is introduced, where t is time and V_0 the group velocity of the carrier wave. The temporal variable is rescaled by pulse duration τ_0 , i.e., it is taken as $\tau = T/\tau_0$. Thus, $\nabla^2 = \nabla_{x,y,\tau}^2 \equiv \partial^2/\partial x^2 + \partial^2/\partial y^2 + \partial^2/\partial \tau^2$ is the corresponding spatiotemporal Laplacian, where $\partial^2/\partial \tau^2$ accounts for the temporal dispersion (which must be anomalous to have to right sign) [56,57].

Coefficients γ_1 and γ_2 in Eq. (1) represent the cubic and quintic nonlinearities of the media, respectively. To achieve the soliton-supporting balance between the dispersion, diffraction and nonlinearities, $\gamma_1 > 0$ and $\gamma_2 < 0$ are necessary. The last term of Eq. (1) is the external potential with strength p (the lattice depth). The modulated Bessel lattice is defined as

$$V(x, y) = J_{n_J}^2(\sqrt{2\beta}r)\cos^2(n\varphi), \quad (2)$$

where J_{n_J} is the Bessel function of order n_J , $r = \sqrt{x^2 + y^2}$ is the radial coordinate, $\beta^{-1/2}$ is the radial lattice scale, while φ and n are the azimuthal angle and azimuthal index, respectively [58,59]. In this work, we consider the most natural case, with equal Bessel and azimuthal indices, $n_J = n$. The potential defined by Eq. (2) with $n = 2$ and 3 are shown in Figs. 1(b) and (c), respectively. The number of the angular harmonic of the lattice potential is $2n$. The Bessel-lattice potential can be adjusted by tuning its depth p in Eq. (1). However, this possibility is impeded in available optical crystals, particularly when it is necessary to make the lattice with $n = 1$ very deep. A feasible solution is adopting higher-order Bessel lattices, which possess the capability to mitigate the azimuthal instability inherent in VSs [60]. The following discussion focuses on VSs carrying different topological

charges, supported by higher-order Bessel lattices with the self-focusing cubic and self-repulsive quintic nonlinearities.

Several types of stable solitons have been previously predicted in Bessel lattices [49,61,62]. Experimentally, one can photo-induce the well-defined Bessel optical lattice potential by coupling a pump modulated Bessel beam with the ordinary polarization into a photorefractive crystal, while launching a soliton as a probe beam with the extraordinary polarization [63]. Taking the strontium-barium niobate crystal as an example, one concludes that the width of the pump beam, carried by wavelength $\lambda = 632$ nm, should be around $r_0 = 10$ μm, the respective scaled propagation distance $z = 1$ in Eq. (1) corresponding to ~ 1 mm of the actual crystal length [62].

3. The results and discussions

3.1. The numerical method

Stable solutions of Eq. (1) for a probe beam propagating along the z axis can be sought for as $\psi = \phi(x, y)e^{ibz}$, where $\phi(x, y)$ is the stationary waveform, and b the real propagation constant. The input is selected as a Gaussian beam multiplying the vortical phase dislocation with integer winding number (topological charge) $m \geq 0$:

$$\phi(x, y) = A \exp\left(-\frac{r^2}{w^2}\right) r^m e^{im\varphi}, \quad (3)$$

where we fix the amplitude and width of the input laser beam as $A = 1$ and $w = 0.5$ (corresponding to 5 μm in physical units), respectively. Substituting this input in the stationary version of Eq. (1) and using the modified square-operator method [64], stationary solutions for VSs can be obtained numerically. The power (2D norm) of the spatial solitons is defined as $U = \iint |\psi|^2 dx dy$, and the energy (3D norm) of VLBs is $U = \iiint |\psi|^2 dx dy d\tau$.

The evolution of VSs is performed by direct simulations of the full (z -dependent) equation (1) using the split-step Fourier method. The stability of the VS modes is evaluated by the fidelity [65], which is defined as

$$J(z) = \frac{|\iint \psi(x, y, z) |\psi(x, y, z=0)| dx dy|^2}{\iint |\psi(x, y, z)|^2 dx dy \cdot \iint |\psi(x, y, z=0)|^2 dx dy}, \quad (4)$$

J remaining close to 1 implying high fidelity. In this work, 5% white noise is added in the propagation evolution to simulate the noise of the real physics. Stable solitons are defined as ones that propagate keeping high fidelity ($J \geq 0.9$) up to $z = 500$ (about 500 mm in physical units).

3.2. The modulation and dynamics of 2D VSs

The profiles of VSs obtained for various integer values of n , which represents the order of the Bessel lattice and azimuthal-modulation index, are depicted in Fig. 2. The results indicate that, with the increase of n , cores of individual lobes merge to form a ring-like structure, which is common for vortex structures, as exemplified in Figs. 2(e) and 2(f) for $n = 5$ and 6, respectively. The phase distribution consistently demonstrates vortex characteristics with topological charge $m = 1$ [corresponding to $m = 1$ in Eq. (3)], regardless of whether the intensity distribution of the VSs exhibits a multi-core or nearly-axisymmetric vortex structure.

In the present system, VSs with high topological charges up to $m = 6$ can be generated too, as shown in Fig. 3. Here the order of the Bessel lattice is $n = 6$ and, accordingly, the number of the individual cores is 12. Specifically, when $m = 1$ and 2, the cores fuse and form a ring structure, presenting a conventional vortex pattern, as shown in Fig. 3(a) and 3(b). As m increases to 3 or 4, the cores of the VSs start to separate, revealing a distinct 12-core structure, as shown in Figs. 3(c) and 3(d). However, when m attains values 5 and 6, the cores start to split in the course of the propagation, as a result of the azimuthal instability, cf. Refs. [11,12]. The stability of these VSs with different topological charges m is reported below.

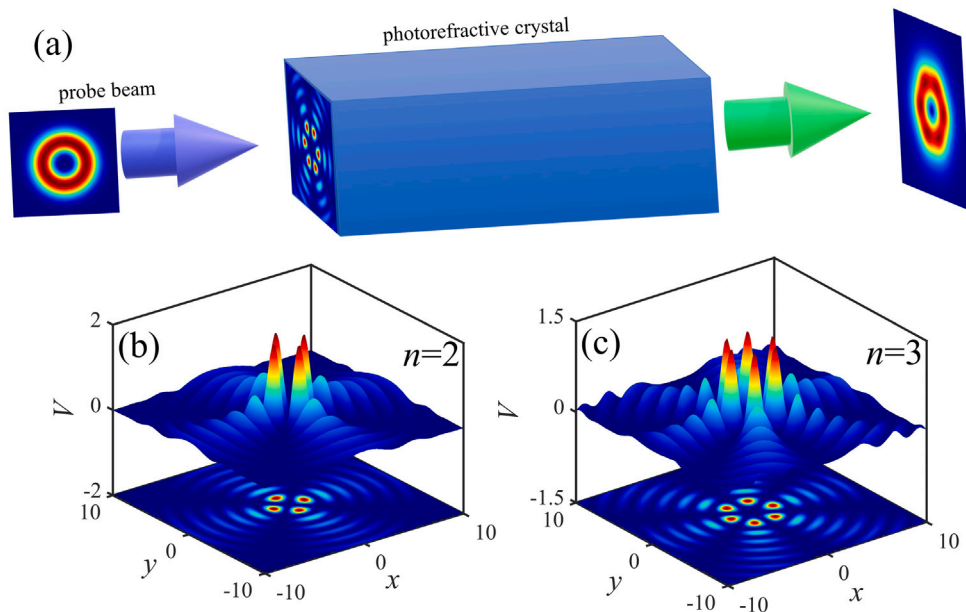


Fig. 1. (a) The scheme of cubic-quintic nonlinear medium with the photon induced Bessel lattice. (b, c) The potential induced by the n -th-order Bessel lattice with azimuthal indices $n = 2$ and 3 , respectively.

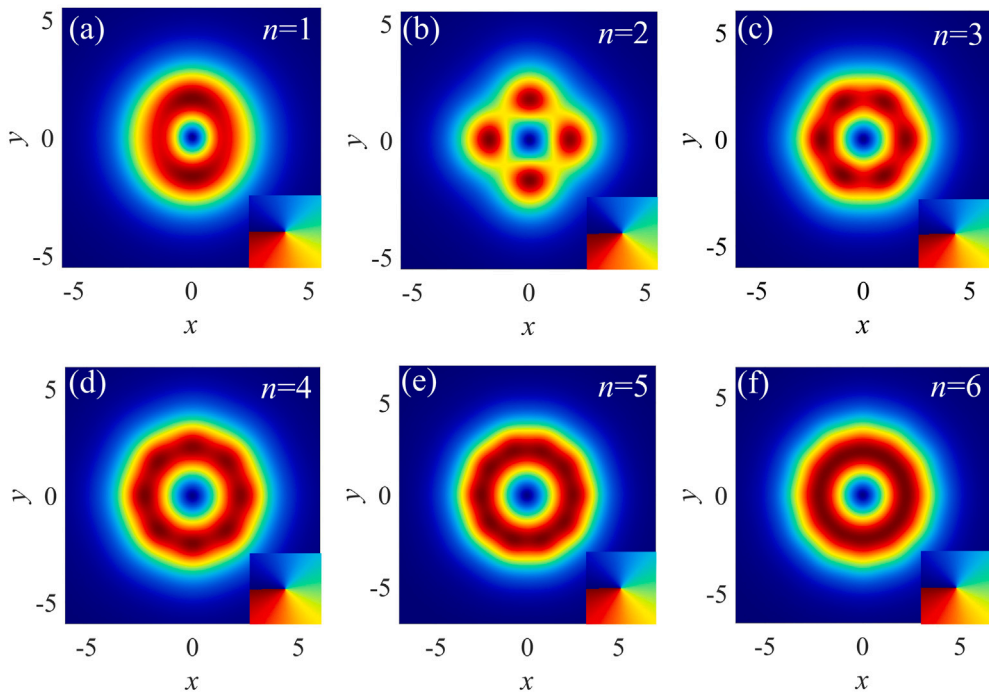


Fig. 2. Stable vortex solitons with different values of the modulation index n of the Bessel-lattice potential [see Eq. (2)], from $n = 1$ to 6 , as indicated in the panels. The other parameters are $(m, p, b, \gamma_1, \gamma_2) = (1, 5, 0.7, 8, -2)$.

It is obvious that the radius of VSs, which is defined as $R = \sqrt{\iint (x^2 + y^2) |\psi|^2 dx dy} / \iint |\psi|^2 dx dy$, increases with the increase of the topological charge. Numerical results show that the radii are $R = 1.2402, 2.3032, 3.3661, 3.9567, 4.4291$, and 4.6654 for vortices with topological charges $m = 1$ through 6 , respectively. The change of the radius is mainly caused by the centrifugal force resulting from the orbital angular momentum. The phase structure consistently exhibits vortex characteristics and agrees with the integer value of topological charge m .

For the 6-order Bessel lattice, dependences of characteristics of VSs on parameters are presented in Fig. 4. Figs. 4(a) and 4(b) display the

$U(b)$ relation, for power U , with various fixed values of topological charge m and potential strength p , respectively. It is found that U increases monotonously with b , meaning that the VS solutions satisfy the well-known Vakhitov-Kolokolov criterion [66,67], which is the necessary stability criterion. Additionally, the stability ranges of VSs with lower topological charges ($m = 1$) are much larger than for higher charges ($m = 3$). Note that the power decreases with the increase of the potential's strength p , while the stability ranges do not change in this case, as shown in Fig. 4(b).

The contributions of cubic and quintic nonlinearities, $\gamma_1 > 0$ and $\gamma_2 < 0$ are compared in Figs. 4(c) and (d), respectively, the size of γ_1

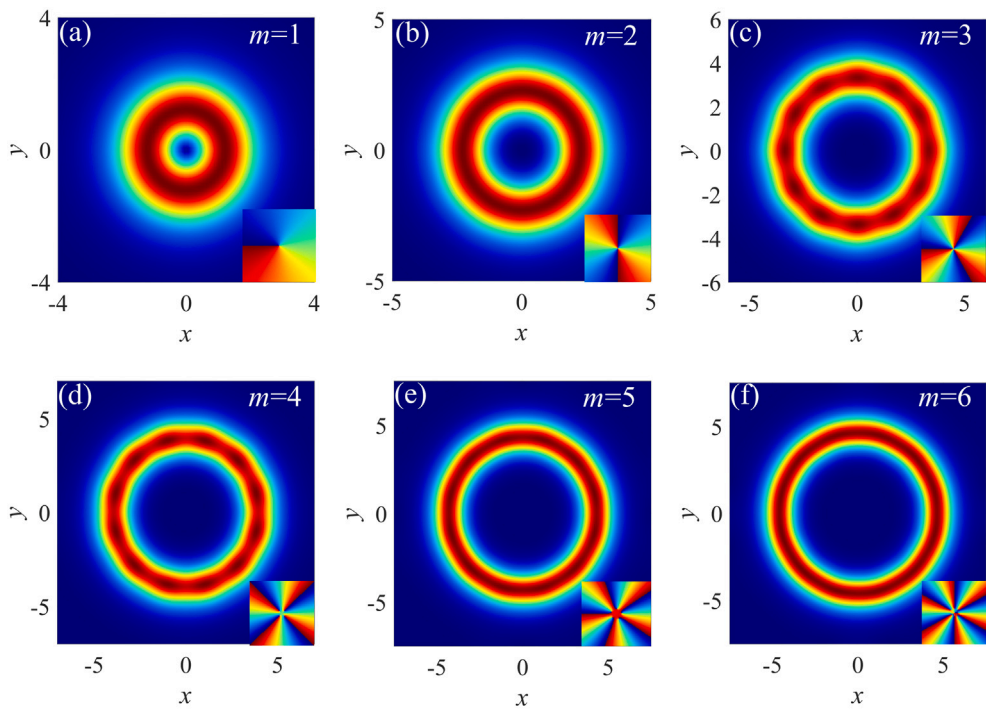


Fig. 3. Vortex solitons with topological charges $m = 1\text{--}6$ [see Eq. (3)]. The other parameters are $(n, p, b, \gamma_1, \gamma_2) = (6, 1, 0.9, 6, -1)$. VSSs with $m = 1\text{--}3$ can propagate stably which will be discussed in Fig. 5.

being essentially larger than that of γ_2 . Here, the parameters γ_1 and γ_2 represent the different responses of refractive index to light intensity. The relations $\gamma_1 > 0$ and $\gamma_2 < 0$ correspond to the self-focusing cubic and self-repulsive quintic nonlinearities of media adopted in this work. The amplitude of γ_2 is rather smaller than γ_1 . This result indicates that the cubic nonlinearity is the primary factor contributing to the stabilization of VSSs when the light intensity is relatively low, while the effect of the quintic nonlinearity is, naturally, more pronounced for higher intensity. Note that the power of VSSs decreases monotonously with the increase of both γ_1 and γ_2 (note that the increase of $\gamma_2 < 0$ implies the decrease of $|\gamma_2|$).

The stability of these VSSs is evaluated by monitoring fidelity (4) in the course of the propagation along the z coordinate, as shown in Fig. 5 for topological charges $m = 1\text{--}6$. It is found that the distance of the stable propagation decreases with the increase of m . Specifically, the VSSs keep values $J > 0.95$ within $0 < z < 1800$ for $m = 1$ [Fig. 5(a)], and $0 < z < 1100$ for $m = 2$. The distance at which the fidelity drops to $J = 0.9$ is 798, 379, 241, and 165 for $m = 3, 4, 5$ and 6, respectively. Thus, VSSs with $m = 1, 2, 3$ can be considered as, practically speaking, fully stable modes.

The stability domains of VSSs with various topological charges in the (γ_1, γ_2) and (p, b) planes are presented in Fig. 6. It is found that the domains in the (γ_1, γ_2) plane are similar for different topological charges m , as seen in Figs. 6(a, b, c). The stability ranges of the variation of the cubic nonlinearity coefficient γ_1 are larger than that for the quintic one γ_2 . In the (p, b) plane, VSSs with lower topological charges have a larger stability domain than their counterparts with higher m , as seen in Figs. 6(d, e, f). This is in agreement with the results reported in Fig. 4.

3.3. Ring- and necklace-shaped vortex light bullets (VLBs)

Adding the temporal coordinate and dispersion to the underlying NLSE, profiles of the respective spatiotemporal modes, in the form of VLBs with $n = 1\text{--}6$, are presented in Fig. 7. The number of local cores in VLBs, produced by potential (2), is $2n$, i.e., the same as in the corresponding 2D VSSs. When n is relatively small, the profile of VLBs

features a necklace-like shape. With the increase of n , the cores merge into a ring-shaped profile.

The profiles of VLBs with topological charges $m = 1\text{--}6$ are shown in Fig. 8. It is found that the distribution of the absolute value $|\psi|$ and phase structure in the (x, y) plane at $\tau = 0$ are consistent with the respective 2D VSSs. Similar to the 2D VSSs, the radius of VLBs at $\tau = 0$ increases with the increase of the topological charge. Although the VLBs with high topological charges ($m \geq 4$) can be generated, they quickly split in the course of the propagation. Examples of the propagation of stable ($m = 1$) and unstable ($m = 6$) VLBs are shown in Figs. 9 and 10, respectively.

Dependences of the VLBs' energy on the parameters, such as b, m, p, γ_1 , and γ_2 , are presented in Fig. 11. It is seen that the energy increases monotonously with propagation constant b , hence the 3D VLBs also satisfy the above-mentioned Vakhitov–Kolokolov criterion [66,67]. On the other hand, the energy decreases with the increase of both cubic (γ_1) and quintic (γ_2) nonlinearity coefficients. These results are similar to those displayed above for 2D VSSs, cf. Fig. 4, a difference being that the $U(b)$ dependence is very weakly affected by the variation of lattice depth p .

4. Conclusion

In this work, we have proposed a scheme for the study of the existence, stability, and evolution of 2D VSSs (spatial vortex solitons) and 3D VLBs (spatiotemporal vortex light bullets) under the action of the competing cubic–quintic (focusing–defocusing) nonlinearities and azimuthally modulated Bessel lattices, with the angular-modulation index n equal to the order of the Bessel function. By dint of numerical calculations, we have identified stable multicore 2D VSSs and 3D VLBs with topological charges $m = 1, 2$, and 3. Our results demonstrate that the size of multicore VSSs and VLBs increases with the growth of m . The number of cores in these states is determined by the modulation index n , leading to the formation of ring- and necklace-shaped profiles. The effect of the cubic nonlinearity on VSSs is greater than that of the quintic term in the case of relatively low light intensity. The results offer a novel approach for the creation of stable VSSs and VLBs with

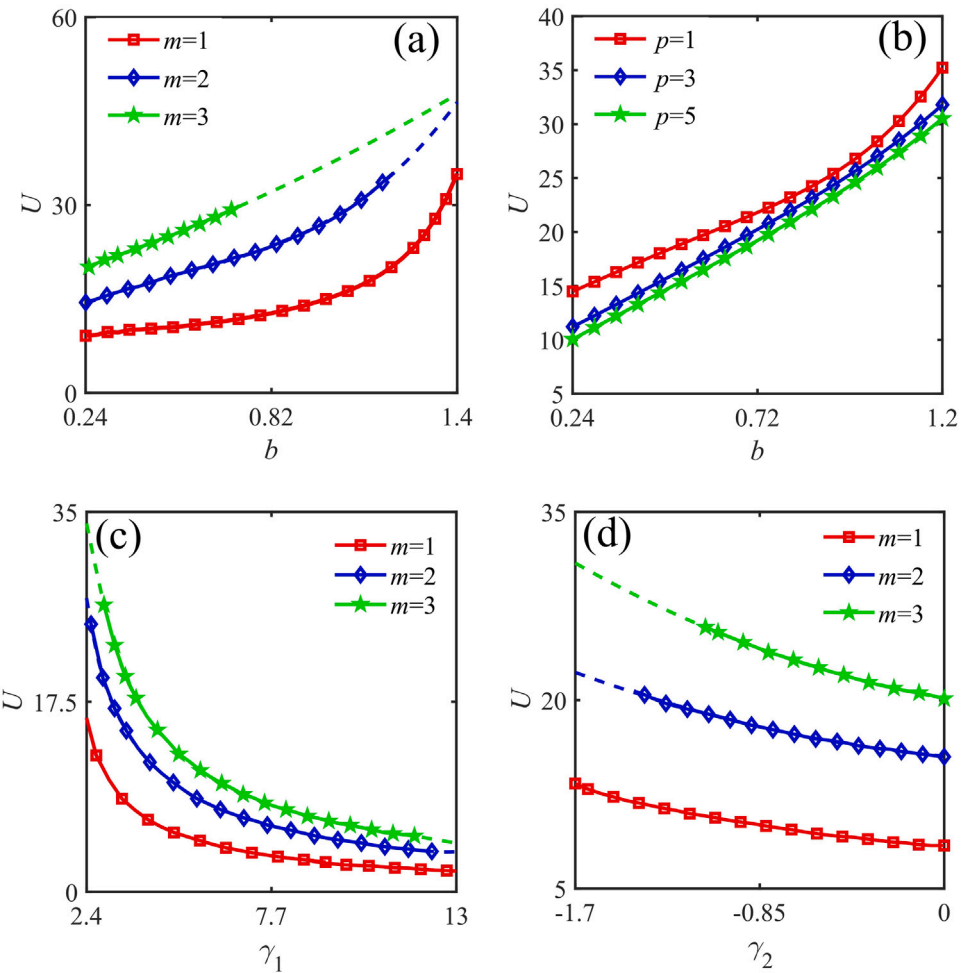


Fig. 4. The VS power as the function of control parameters b , γ_1 , and γ_2 . In each panel, cases with different topological charges m or lattice depth p are displayed for the comparison. The fixed parameters in all panels are $(n, m, b, p, \gamma_1, \gamma_2) = (6, 1, 0.5, 1, 5, -1)$.

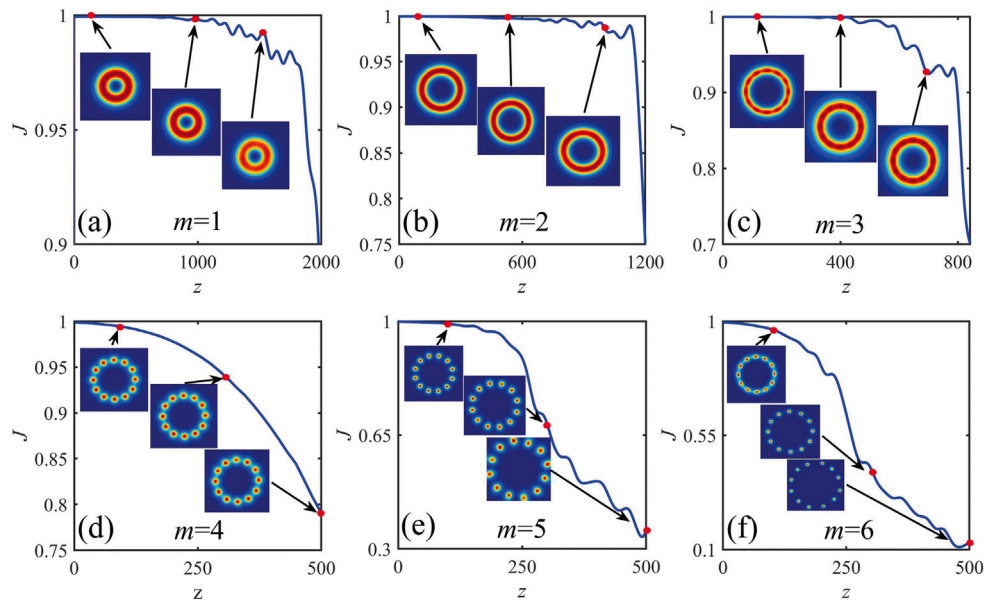


Fig. 5. Fidelity J of VSs [see Eq. (4)] with topological charges $m = 1 - 6$ vs, the propagation distance. 5% white noise is added in the simulation. The insets are profiles of VSs at different values of z . The other parameters are the same as Fig. 4.

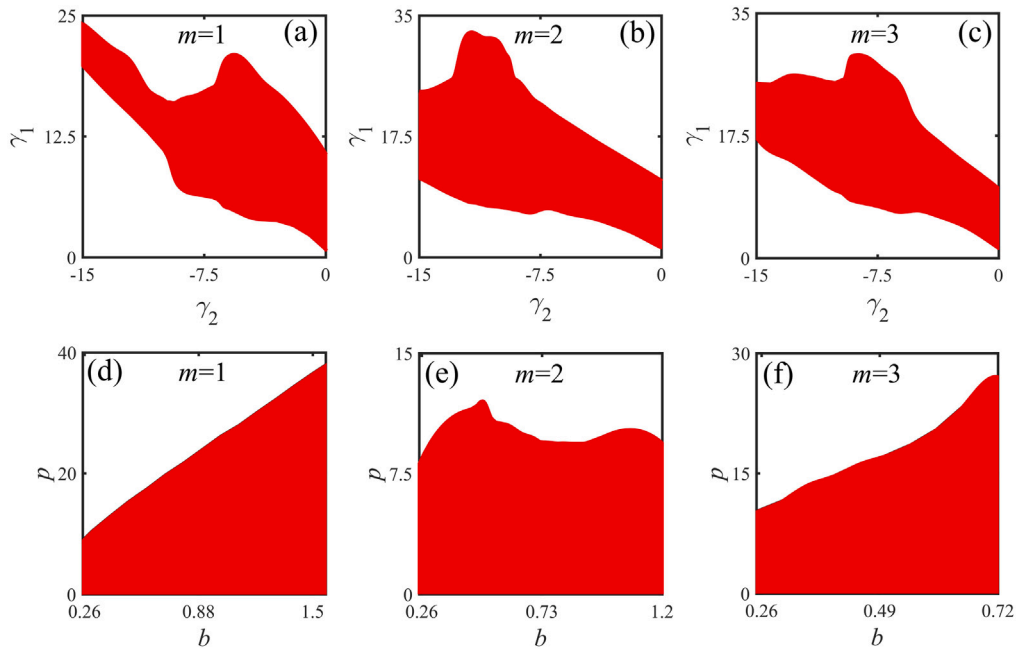


Fig. 6. Stability domains of VSs in the (γ_1, γ_2) and (p, b) planes. The stability domains are painted red. The fixed parameters in all panels are $(n, b, p, \gamma_1, \gamma_2) = (6, 0.5, 1, 5, -1)$.

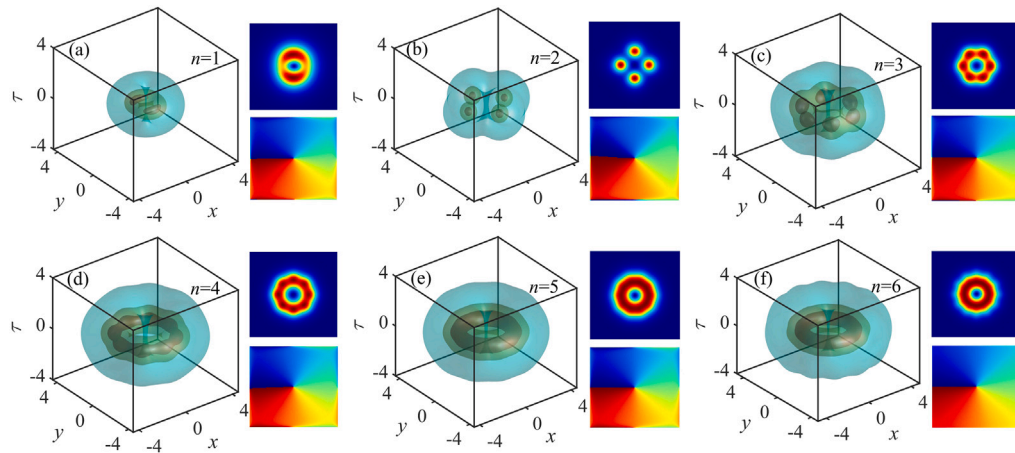


Fig. 7. Vortex VLBS with different orders of the Bessel lattice, $n = 1-6$. The isosurface of the absolute value of the wave function is shown in each panel, along with the projection and phase structure in the (x, y) plane. The other parameters are $(m, p, b, \gamma_1, \gamma_2) = (1, 5, 1, 5, -1)$.

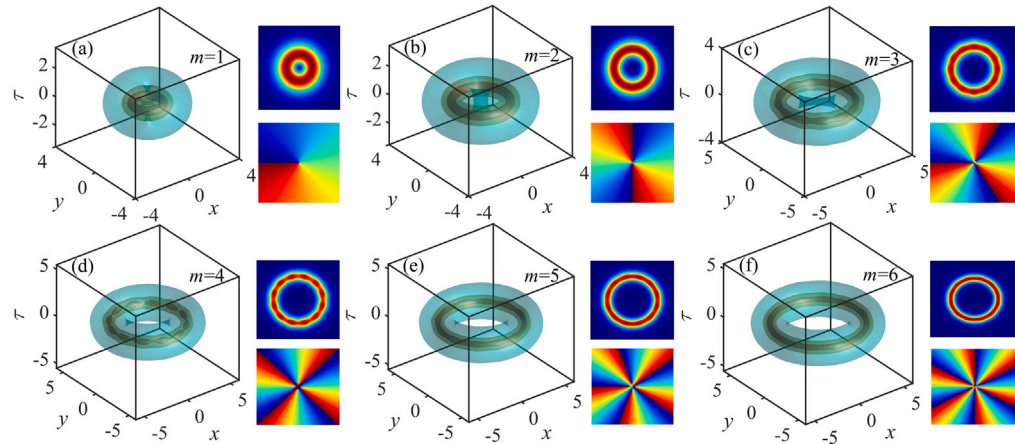


Fig. 8. VLBS with different topological charges $m = 1-6$, see Eq. (3). The insets show the absolute value $|\psi|$ and phase structure in the (x, y) plane. The other parameters are $(n, p, b, \gamma_1, \gamma_2) = (6, 2, 1, 5, -1)$. Radii of VLBS with $m = 1-6$ are 0.9647, 1.7811, 2.8942, 3.480, 3.9332, and 4.2548, respectively.

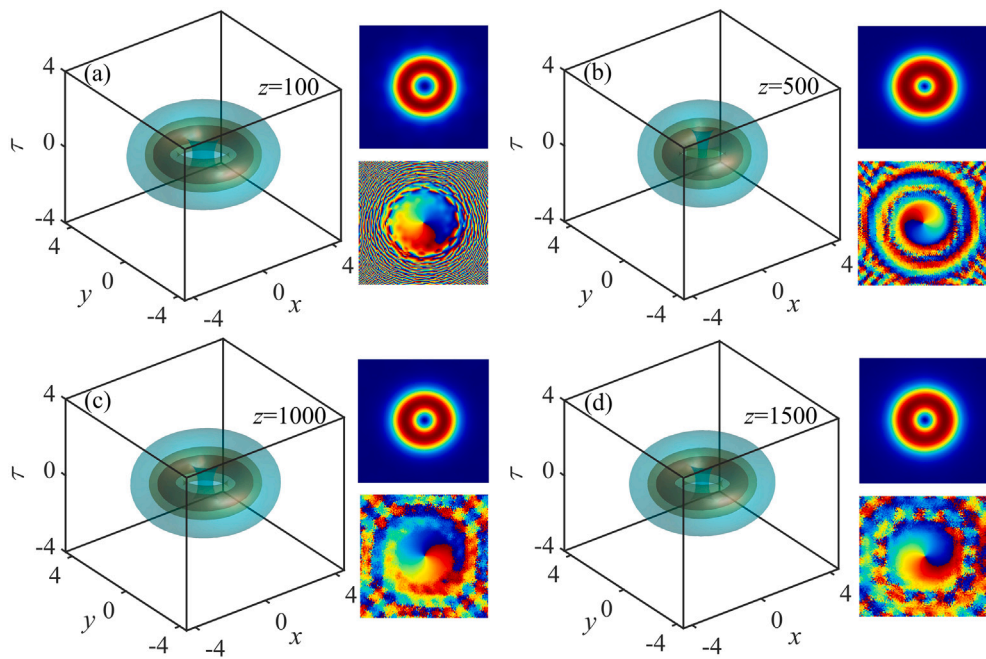


Fig. 9. The stable propagation of VLB with $m = 1$. The parameters are the same as Fig. 8(a).

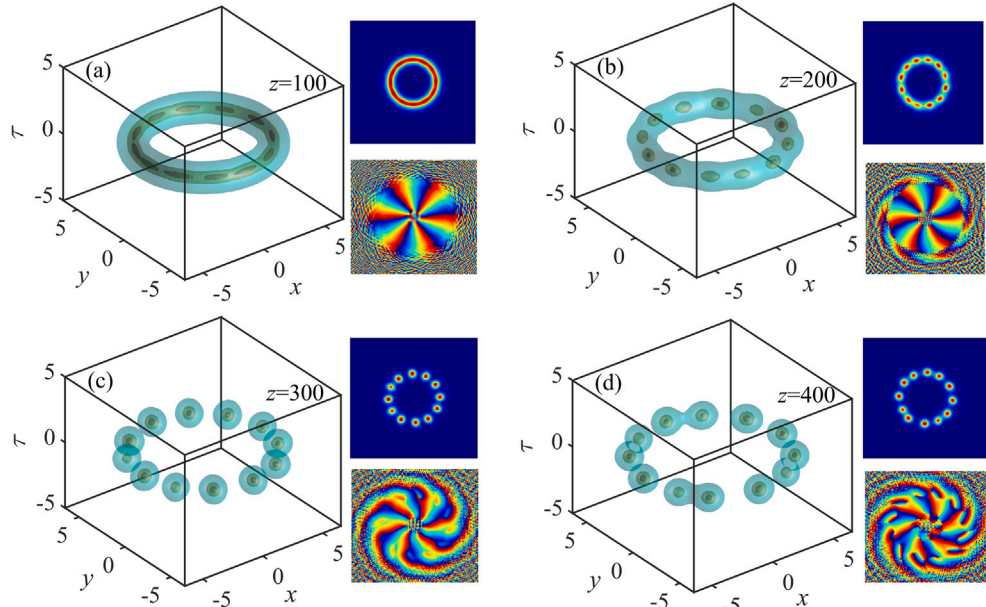


Fig. 10. The unstable propagation of VLB with $m = 6$. The parameters are the same as Fig. 8(f).

higher topological charges. These findings contribute to the broader understanding of nonlinear optical phenomena and suggest potential applications to optical communications, imaging, and data processing.

CRediT authorship contribution statement

Di Wu: Resources, Methodology. **Junhao Li:** Methodology, Investigation. **Xi Gao:** Data curation. **Yi Shi:** Supervision. **Yuan Zhao:** Writing – original draft. **Liangwei Dong:** Writing – review & editing. **Boris A. Malomed:** Writing – review & editing. **Ni Zhu:** Writing – original draft, Conceptualization. **Siliu Xu:** Writing – review & editing, Funding acquisition.

Declaration of competing interest

The authors declare that they have no known competing financial interests or personal relationships that could have appeared to influence the work reported in this paper.

Acknowledgments

This work was supported by the National Natural Science Foundation of China (62275075), Natural Science Basic Research Program in Shaanxi Province of China (2022JZ-02), Natural Science Foundation of Hubei Province (2023AF042), Training Program of Innovation and Entrepreneurship for Undergraduates of Hubei Province (S202410927046, S202210927003), and Israel Science Foundation (grant No. 1695/22).

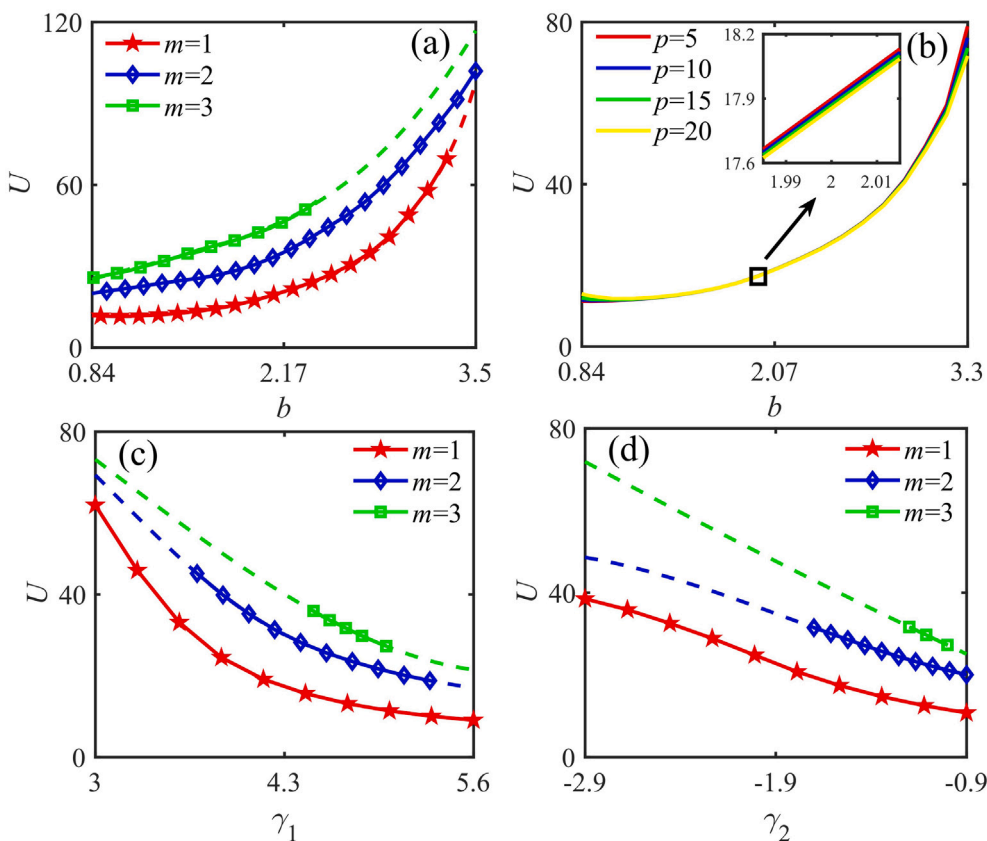


Fig. 11. The dependence of the VLBs' energy on parameters b and $\gamma_{1,2}$. The fixed parameters are $(b, m, n, p, \gamma_1, \gamma_2) = (1, 1, 6, 15, 5, -1)$.

Data availability

Data will be made available on request.

References

- [1] Kivshar YS, Agrawal GP. Optical solitons: from fibers to photonic crystals. San Diego: Academic; 2003.
- [2] Akhmediev NN, Ankiewicz A. Solitons. London: Chapman-Hall; 1997.
- [3] Donadello S, Serafini S, Tylutki M, Pitaevskii LP, Dalfovo F, Lamporesi G, et al. Observation of solitonic vortices in Bose-Einstein condensates. *Phys Rev Lett* 2014;113:065302.
- [4] Li Y, Liu Y, Fan Z, Pang W, Fu S, Malomed BA. Two-dimensional dipolar gap solitons in free space with spin-orbit coupling. *Phys Rev A* 2017;95:063613.
- [5] Liao B, Li S, Huang C, Luo Z, Pang W, Tan H, et al. Anisotropic semivortices in dipolar spinor condensates controlled by Zeeman splitting. *Phys Rev A* 2017;96:043613.
- [6] Li G, Zhao Z, Jiang X, Chen Z, Liu B, Malomed BA, et al. Strongly anisotropic vortices in dipolar quantum droplets. *Phys Rev Lett* 2024;133:053804.
- [7] Li G, Jiang X, Liu B, Chen Z, Malomed BA, Li Y. Two-dimensional anisotropic vortex quantum droplets in dipolar Bose-Einstein condensates. *Front Phys* 2024;19:22202.
- [8] Zhang X, Xu X, Zheng Y, Chen Z, Liu B, Huang C, et al. Semidiscrete quantum droplets and vortices. *Phys Rev Lett* 2019;123:133901.
- [9] Sonin EB. Vortex oscillations and hydrodynamics of rotating superfluids. *Rev Modern Phys* 1987;59:87–155.
- [10] Verbeeck J, Tian H, Schattschneider P. Production and application of electron vortex beams. *Nature* 2010;467:301–4.
- [11] Torner L, Petrov DV. Azimuthal instabilities and self-breaking of beams into sets of solitons in bulk second-harmonic generation. *Electron Lett* 1997;33:608.
- [12] Kartashov YV, Vysloukh VA, Torner L. Stable ring-profile vortex solitons in bessel optical lattices. *Phys Rev Lett* 2005;94:043902.
- [13] Petrov DV, Torner L, Martorell J, Vilaseca R, Torres JP, Cojocaru C. Observation of azimuthal modulational instability and formation of patterns of optical solitons in a quadratic nonlinear crystal. *Opt Lett* 1998;23:1444.
- [14] Bigelow MS, Zerom P, Boyd RW. Breakup of ring beams carrying orbital angular momentum in sodium vapor. *Phys Rev Lett* 2004;92:083902.
- [15] Malomed BA. Multidimensional solitons. Melville, New York: American Institute of Physics Publishing; 2022.
- [16] Malomed BA. Multidimensional soliton systems. *Adv Phys X* 2024;9:2301592.
- [17] Mihalache D. Localized structures in optical media and Bose-Einstein condensates: An overview of recent theoretical and experimental results. *Rom Rep Phys* 2024;76:402.
- [18] Zhao F, Xu X, He H, Zhang L, Zhou Y, Chen Z, et al. Vortex solitons in Quasi-Phase-Matched photonic crystals. *Phys Rev Lett* 2023;130:157203.
- [19] Chen S, Zhou B, Jiao Y, Wang L, Zhao Y, Xu S. Vortex solitons in rotating Quasi-Phase-Matched photonic crystals. *Opt Express* 2024;32:39963.
- [20] Xu X, Zhao F, Huang J, He H, Zhang L, Chen Z, et al. Semidiscrete optical vortex droplets in quasi-phase-matched photonic crystals. *Opt Express* 2023;31:38343.
- [21] He J-R, Jiao Y, Zhou B, Zhao Y, Fan Z, Xu S. Vortex light bullets in rotating Quasi-Phase-Matched photonic crystals. *Chaos Solitons Fractals* 2024;188:115514.
- [22] Li Y, Yesharim O, Hurvitz I, Karniel A, Fu S, Porat G, et al. Adiabatic geometric phase in fully nonlinear three-wave mixing. *Phys Rev A* 2020;101:033807.
- [23] Zhao F, Lu J, He H, Zhou Y, Fu S, Li Y. Geometric phase with full-wedge and half-wedge rotation in nonlinear frequency conversion. *Opt Express* 2021;29:21820.
- [24] Karniel A, Li Y, Arie A. The geometric phase in nonlinear frequency conversion. *Front Phys* 2022;17:12301.
- [25] Mihalache D, Mazilu D, Crasovan L-C, Towers I, Malomed BA, Buryak AV, et al. Stable three dimensional spinning optical solitons supported by competing quadratic and cubic nonlinearities. *Phys Rev E* 2002;66:016613.
- [26] Quiroga-Teixeiro M, Michinel H. Stable azimuthal stationary state in quintic nonlinear optical media. *J Opt Soc Am B* 1997;14:2004.
- [27] Zhu X, Cai Z, Liu J, Liao S, He Y. Spatial solitons in non-parity-time-symmetric complex potentials with competing cubic-quintic nonlinearities. *Nonlinear Dynam* 2022;108:2563.
- [28] Raghavan S, Agrawal GP. Spatiotemporal solitons in inhomogeneous nonlinear media. *Opt Commun* 2000;180:377.
- [29] Ferrando A, Zácarés M, Fernández de Córdoba P, Binosi D, Monsoriu JA. Vortex solitons in photonic crystal fibers. *Opt Express* 2004;12:817.
- [30] Yang J, Musslimani ZH. Fundamental and vortex solitons in a two-dimensional optical lattice. *Opt Lett* 2003;28:2094.
- [31] Dong L, Ye F. Shaping solitons by lattice defects. *Phys Rev A* 2010;82:053829.
- [32] Zhao Y, Lei Y-B, Xu Y-X, Xu S-L, Triki H, Biswas A. Vector spatiotemporal solitons and their memory features in cold Rydberg gases. *Chin Phys Lett* 2022;39:034202.

- [33] Bai Z, Li W, Huang G. Stable single light bullets and vortices and their active control in cold Rydberg gases. *Optica* 2019;6:309.
- [34] Guo Y-W, Xu S-L, He J-R, Deng P, Belić MR, Zhao Y. Transient optical response of cold Rydberg atoms with electromagnetically induced transparency. *Phys Rev A* 2020;101:023806.
- [35] Li B-B, Zhao Y, Xu S-L. Two-dimensional gap solitons in parity-time symmetry moiré optical lattices with Rydberg–Rydberg interaction. *Chin Phys Lett* 2023;40:044201.
- [36] Reyna AS, Boudebs G, Malomed BA, Araújo CBD. Robust self-trapping of vortex beams in a saturable optical medium. *Phys Rev A* 2016;93:013840.
- [37] Reyna AS, Baltar HTMC, Bergmann E, Amaral AM, Falcão-Filho EL, Brevet PF, et al. Observation and analysis of creation, decay, and regeneration of annular soliton clusters in a lossy cubic quintic optical medium. *Phys Rev A* 2020;102:033523.
- [38] Abo-Shaeer JR, Raman C, Vogels JM, Ketterle W. Observation of vortex lattices in Bose–Einstein condensates. *Science* 2001;292:476.
- [39] Mandel O, Greiner M, Widera A, Rom T, Hänsch T, Bloch I. Controlled collisions for multi-particle entanglement of optically trapped atoms. *Nature* 2003;425:937.
- [40] Wang X, Chen Z. Observation of discrete solitons and soliton rotation in optically induced periodic ring lattices. *Phys Rev Lett* 2006;96:083904.
- [41] Xu S, Li J, Hou Y, He JR, Fan Z, Zhao Y, et al. Vortex light bullets in rydberg atoms trapped in twisted \mathcal{PT} -symmetric waveguide arrays. *Phys Rev A* 2024;110:023508.
- [42] Zhao Y, Huang Q, Gong T, Xu S, Li Z, Malomed BA. Three-dimensional solitons supported by the spin–orbit coupling and rydberg-rydberg interactions in \mathcal{PT} -symmetric potentials. *Chaos Solitons Fractals* 2024;187:115329.
- [43] Wang Q, Mihalache D, Belić MR, Zeng L, Lin J. Spiraling Laguerre–Gaussian solitons and arrays in parabolic potential wells. *Opt Lett* 2023;48:4233–6.
- [44] Wang Q, Mihalache D, Belić MR, Lin J. Mode conversion of various solitons in parabolic and cross-phase potential wells. *Opt Lett* 2024;49:1607–10.
- [45] Mihalache D, Mazilu D, Lederer F, Malomed BA, Kartashov YV, Crasovan L-C, et al. Stable spatiotemporal solitons in Bessel optical lattices. *Phys Rev Lett* 2005;95:023902.
- [46] Vasara A, Turunen J, Friberg A. General diffraction-free fields produced by computer-generated holograms. *J Opt Soc Amer A* 1989;6:1748.
- [47] Arlt J, Dholakia K. Generation of high-order Bessel beams by use of an axicon. *Opt Commun* 2000;177:297.
- [48] Fischer R, Neshev DN, Lopez-Aguayo S, Desyatnikov AS, Sukhorukov AA, Krolkowski W, et al. Light localization in azimuthally modulated Bessel photonic lattices. *J Mater Sci Mater Electron* 2007;18:S277.
- [49] Fischer R, Neshev DN, Lopez-Aguayo S, Desyatnikov AS, Sukhorukov AA, Krolkowski W, et al. Observation of light localization in modulated Bessel optical lattices. *Opt Express* 2006;14:2825.
- [50] Li H, Xu S-L, Belić MR, Cheng J-X. Three-dimensional solitons in Bose–Einstein condensates with spin–orbit coupling and Bessel optical lattices. *Phys Rev A* 2018;98:033827.
- [51] Xu S-L, Zhou Q, Zhao D, Belić MR, Zhao Y. Spatiotemporal solitons in cold rydberg atomic gases with Bessel optical lattices. *Appl Math Lett* 2020;106:106230.
- [52] Ye F, Kartashov YV, Hu B, Torner L. Light bullets in Bessel optical lattices with spatially modulated nonlinearity. *Opt Express* 2009;17:11328.
- [53] Jin L, Hang C, Huang G. Multidimensional optical solitons and their manipulation in a cold atomic gas with a parity-time-symmetric optical bessel potential. *Phys Rev A* 2023;107:053501.
- [54] Chen J, Song J, Zhou Z, Yan Z. Data-driven localized waves and parameter discovery in the massive thirring model via extended physics-informed neural networks with interface zones. *Chaos Solitons Fractals* 2023;176:114090.
- [55] Qiu WX, Geng KL, Zhu BW, Liu W, Dai CQ. Data-driven forward-inverse problems of the 2-coupled mixed derivative nonlinear Schrödinger equation using deep learning. *Nonlinear Dynam* 2024;112:10215.
- [56] Desyatnikov A, Maimistov A, Malomed B. Three-dimensional spinning solitons in dispersive media with the cubic-quintic nonlinearity. *Phys Rev E* 2000;61:3107.
- [57] Towers I, Buryak AV, Sammut RA, Malomed BA, Crasovan LC, Mihalache D. Stability of spinning ring solitons of the cubic-quintic nonlinear Schrödinger equation. *Phys Lett A* 2001;288:292.
- [58] Zheng J, Dong L. Multipeaked fundamental and vortex solitons in azimuthally modulated Bessel lattices. *J Opt Soc Am B* 2011;28:780.
- [59] Dong L, Wang H, Zhou W, Yang X, Lv X, Chen H. Necklace solitons and ring solitons in Bessel optical lattices. *Opt Express* 2008;16:5649.
- [60] Dong L, Ye F, Wang H. Suppression of azimuthal instability of ring vortex solitons. *New J Phys* 2009;11:073026.
- [61] Kartashov YV, Egorov AA, Vysloukh VA, Torner L. Stable soliton complexes and azimuthal switching in modulated Bessel optical lattices. *Phys Rev E* 2004;70:065602.
- [62] Kartashov YV, Ferrando A, Egorov AA, Torner L. Soliton topology versus discrete symmetry in optical lattices. *Phys Rev Lett* 2005;95:123902.
- [63] Kartashov YV, Carretero-Gonzalez R, Malomed BA, Vysloukh VA, Torner L. Multipole-mode solitons in Bessel optical lattices. *Opt Express* 2005;13:10703.
- [64] Yang J, Lakoba TI. Universally-convergent squared-operator iteration methods for solitary waves in general nonlinear wave equations. *Stud Appl Math* 2007;118:153.
- [65] Hang C, Li W, Huang G. Nonlinear light diffraction by electromagnetically induced gratings with \mathcal{PT} symmetry in a Rydberg atomic gas. *Phys Rev A* 2019;100:043807.
- [66] Vakhitov NG, Kolokolov AA. Stationary solutions of the wave equation in a medium with nonlinearity saturation. *Radiophys Quantum Electron* 1973;16:783–9. <http://dx.doi.org/10.1007/BF01031343>.
- [67] Bergé L. Wave collapse in physics: principles and applications to light and plasma waves. *Phys Rep* 1998;303:259–370.